Inorg. Chem. **2008**, *47*, 4627−4638

Identification of a Copper(I) Intermediate in the Conversion of 1-Aminocyclopropane Carboxylic Acid (ACC) into Ethylene by Cu(II)−ACC Complexes and Hydrogen Peroxide

Wadih Ghattas,[†] Michel Giorgi,[‡] Yasmina Mekmouche,[†] Tsunehiro Tanaka,[§] Antal Rockenbauer,[||] Marius Réglier,[†] Yutaka Hitomi,*[,§] and A. Jalila Simaan*[,†]

Institut des Sciences Moléculaires de Marseille, ISM²/BiosCiences UMR-CNRS 6263, Aix-Marseille Université, Centre Scientifique de Saint-Jérôme, Service 342, 13397 Marseille cedex 20, France, Spectropôle, Aix-Marseille Université, Centre Scientifique de Saint-Jérôme, Av. Escadrille Normandie-Niémen, 13397 Marseille cedex 20, France, Department of Molecular Engineering, Graduate School of Engineering, Kyoto University, Kyoto Daigaku Katsuta, Kyoto 615-8510, Japan, and Chemical Research Center, Hungarian Academy of Sciences, H-1525 Budapest, P.O. Box 17, Hungary

Received November 22, 2007

Several Cu(II) complexes with ACC (= 1-aminocyclopropane carboxylic acid) or AIB (= aminoisobutyric acid) were prepared using 2,2′-bipyridine, 1,10-phenanthroline, and 2-picolylamine ligands: [Cu(2,2′-bipyridine)(ACC)-(H_2O)](ClO_4) (**1a**), [Cu(1,10-phenanthroline)(ACC)](ClO_4) (**2a**), [Cu(2-picolylamine)(ACC)](ClO_4) (**3a**), and [Cu(2,2′-bipyridine)(AIB)(H_2O)](ClO_4) (**1b**). All of the complexes were characterized by X-ray diffraction analysis. The Cu(II)−ACC complexes are able to convert the bound ACC moiety into ethylene in the presence of hydrogen peroxide, in an "ACC-oxidase-like" activity. A few equivalents of base are necessary to deprotonate H_2O_2 for optimum activity. The presence of dioxygen lowers the yield of ACC conversion into ethylene by the copper(II) complexes. During the course of the reaction of Cu(II)−ACC complexes with H_2O_2, brown species (EPR silent and $\lambda_{max} \approx 435$ nm) were detected and characterized as being the Cu(I)−ACC complexes that are obtained upon reduction of the corresponding Cu(II) complexes by the deprotonated form of hydrogen peroxide. The geometry of the Cu(I) species was optimized by DFT calculations that reveal a change from square-planar to tetrahedral geometry upon reduction of the copper ion, in accordance with the observed nonreversibility of the redox process. *In situ* prepared Cu(I)−ACC complexes were also reacted with hydrogen peroxide, and a high level of ethylene formation was obtained. We propose Cu(I)−OOH as a possible active species for the conversion of ACC into ethylene, the structure of which was examined by DFT calculation.

Introduction

The gaseous plant hormone ethylene regulates many processes of plant development and defense such as pigmentation, fruit ripening, and senescence.[1] It is directly biosynthesized from 1-aminocyclopropane carboxylic acid (ACC),[2] a metabolite of methionine. This last step of ethylene biosynthesis is catalyzed by ACC oxidase (ACCO). The conversion of ACC into ethylene implies a two-electron oxidation in the presence of ferrous ions, dioxygen, and ascorbate (see Scheme 1). The products are ethylene, cyanhydric acid, and carbon dioxide. Oxygen is not incorporated in the products and is probably eliminated as water molecules after reduction.[3]

Scheme 1. Reaction Catalyzed by ACC Oxidase

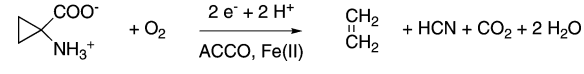

* Authors to whom correspondence should be addressed: E-mail: jalila.simaan@univ-cezanne.fr (A.J.S), hitomi@moleng.kyoto-u.ac.jp (Y.H.).
† ISM²/BiosCiences UMR-CNRS 6263, Aix-Marseille Université.
‡ Spectropôle, Aix-Marseille Université.
§ Kyoto University.
|| Hungarian Academy of Sciences.

(1) Bleecker, A. B.; Kende, H. *Annu. Rev. Cell. Dev. Biol.* **2000**, *16*, 1–18.
(2) Adams, D. O.; Yang, S. F. *Proc. Natl. Acad. Sci. U.S.A.* **1979**, *76*, 170–174.

10.1021/ic702303g CCC: $40.75
Published on Web 04/29/2008

The crystallographic structure of ACCO from *Petunia hybrida* that was recently solved reveals that the active site contains a single Fe(II) ion linked to the side chains of two histidines and one aspartate.[4]

Stereochemical studies have suggested that the conversion of ACC into ethylene proceeds *via* a radical mechanism, and the formation of an aminyl radical was proposed.[5,6] The role of the metal ion in the catalysis remains however unclear. Spectroscopic studies have suggested that, during the first step of the reaction, both ACC and O_2 are coordinated to the iron(II) ion, generating an iron(III)−ACC−superoxo intermediate.[7–9] It has been proposed that the substrate, ACC, is coordinated in a bidentate mode *via* the nitrogen and one oxygen of the carboxylate group. The following steps of the reaction could involve intermediates such as iron−peroxo or high-valent iron−oxo species.[10] The precise catalytic mechanism of ethylene formation and the regeneration of the enzyme in its active Fe(II) state remain however to be elucidated.

To our knowledge, no structural data are available on iron−ACC complexes. Moreover, there are only a few reported functional models of ACCO. In 1985, Baldwin and co-workers reported the oxidation of ACC into ethylene by several transition metal oxidants such as copper(II), permanganate, and ferrate ions in aqueous solution.[6] Several years after, the group of Nishida described several binuclear metal complexes able to convert ACC into ethylene in the presence of an excess of hydrogen peroxide.[11,12] Their Mn(III) and Co(II) complexes exhibited a higher activity than their Fe(III) complexes. However, the conversion yields remained extremely low, and no metal−ACC interaction could be demonstrated.

It thus seems important to obtain structural and reactivity information on metal−ACC complexes. We recently reported the first well-characterized metal−ACC complex, [Cu(ACC)(2,2′-bipyridine)(H_2O)](ClO_4) (**1a**), where ACC is coordinated in a bidentate mode on a copper(II) ion.[13] Shortly after, an original assembly of copper(II) ions bound to two ACC moieties was described by Judas and Raos.[14] We also demonstrated that complex **1a** is able to produce ethylene from the bound ACC moiety in the presence of 10 equiv of hydrogen peroxide.[15] Moreover, the reactivity was strongly dependent on the basicity of the medium, and we noticed that 3 equiv of NaOH were needed in methanol for optimum activity. In these conditions, 67% of the bound ACC was converted into ethylene. We demonstrated that the base had no influence on the initial Cu^{II}−ACC complex since the spectroscopic and spectrometric properties (UV–vis, EPR, ESI-MS) of **1a** remained unchanged upon the addition of up to 5 equiv of NaOH. It rather appeared that it was involved in H_2O_2 deprotonation.

In the present paper, two new Cu(II)−ACC complexes, [Cu(ACC)(1,10-phenanthroline)](ClO_4) (**2a**) and [Cu(ACC)(2-picolylamine)](ClO_4) (**3a**), were prepared and characterized. The reactivity of the different complexes, **1a**, **2a**, and **3a**, with H_2O_2 was studied under various experimental conditions (under air, under nitrogen, and in the presence of radical oxygen species (ROS) scavengers). We describe the identification of brown Cu(I)−ACC species formed during the course of the reaction that were obtained upon reduction of the corresponding Cu(II)−ACC complexes by HOO^-. The Cu(I) redox state of the brown species was determined by spectroelectrochemical experiments. The same reduction also occurred when ACC was replaced by its noncyclic analogue AIB (= aminoisobutyric acid) with the complex [Cu(2,2′-bipyridine)(AIB)(H_2O)](ClO_4), **1b**. Importantly, *in situ* prepared Cu(I)−ACC complexes also produced a high level of ethylene in the presence of hydrogen peroxide. These results indicate the possible involvement of Cu(I)−OOH species in the conversion of ACC into ethylene.

Experimental Procedures

Synthesis. Commercially available chemicals were purchased and used without further purification. **Caution!** *Perchlorate salts are potentially explosive and should be handled with care.*

The syntheses of the copper(II)−ACC and copper(II)−AIB complexes were carried out following a common procedure already described for [Cu(ACC)(2,2′-bipyridine)(H_2O)](ClO_4) (**1a**).[13]

[Cu(AIB)(2,2′-bipyridine)(OH_2)](ClO_4) (1b). The powder was obtained with 75% yield. Anal. Calcd for ($C_{14}H_{18}ClCuN_3O_7$): C, 38.28; H, 4.13; N, 9.57. Found: C 38.30; H, 4.11; N, 9.70.

[Cu(ACC)(1,10-phenanthroline)](ClO_4) (2a). A blue powder was obtained with 95% yield. Anal. Calcd for ($C_{16}H_{14}ClCuN_3O_6$): C, 43.35; H, 3.18; N, 9.48. Found: C, 43.30; H, 3.20; N, 9.45.

[Cu(ACC)(2-picolylamine)](ClO_4) (3a). A violet-blue powder was obtained with 65% yield. Anal. Calcd for ($C_{10}H_{14}ClCuN_3O_6$): C, 32.35; H, 3.80; N, 11.32. Found: C, 32.48; H, 3.52; N, 11.34.

Crystallographic Studies. Single crystals suitable for X-ray crystallography were grown by the slow evaporation of methanol/water solutions of the different complexes. All crystals were mounted on glass fibers. Data for **1af** (CCDC 679692), **2a** (CCDC 631732), and **3a** (CCDC 631731) were collected on a Bruker-Nonius KappaCCD diffractometer at 293 K. Data for **1b** (CCDC 679691) were collected on a Rigaku CCD diffractometer at 293 K. Structures were solved using SIR92, and refinement calculations were performed using SHELX-97. The crystal structure for complex **1a** has been described previously (CCDC 288376).[13]

(3) Costas, M.; Mehn, M. P.; Jensen, M. P. *Chem. Rev.* **2004**, *104*, 939–986.
(4) Zhang, Z.; Ren, J.-S.; Clifton, I. J.; Schofield, C. J. *Chem. Biol.* **2004**, *11*, 1383–1394.
(5) Adlington, R. M.; Baldwin, J. E.; Rawlings, B. J. *J. Chem. Soc., Chem. Commun.* **1983**, 290–292.
(6) Baldwin, J. E.; Jackson, D. A.; Adlington, R. M.; Rawlings, B. J. *J. Chem. Soc., Chem. Commun.* **1985**, 206–207.
(7) Rocklin, A. M.; Tierney, D. L.; Kofman, V.; Brunhuber, N. M. W.; Hoffman, B. M.; Christoffersen, R. E.; Reich, N. O.; Lipscomb, J. D.; Que, L., Jr *Proc. Natl. Acad. Sci. U.S.A.* **1999**, *96*, 7905–7909.
(8) Tierney, D. L.; Rocklin, A. M.; Lipscomb, J. D.; Que, L., Jr.; Hoffman, B. M. *J. Am. Chem. Soc.* **2005**, *127*, 7005–7013.
(9) Zhou, J.; Rocklin, A. M.; Lipscomb, J. D.; Solomon, E. I. *J. Am. Chem. Soc.* **2002**, *124*, 4602–4609.
(10) Rocklin, A. M.; Kato, K.; Liu, H. W.; Lipscomb, J. D. *J. Biol. Inorg. Chem.* **2004**, *9*, 171–182.
(11) Nishida, Y.; Akamatsu, T.; Ishii, T.; Oda, Y. *J. Chem. Soc., Chem Commun.* **1992**, 496–497.
(12) Kobayashi, T.; Sasaki, Y.; Akamatsu, T.; Ishii, T.; Oda, Y.; Masuda, H.; Einaga, H.; Nishida, Y. *Z. Naturforsch., C: J. Biosci.* **1999**, *54*, 534–541.
(13) Ghattas, W.; Gaudin, C.; Giorgi, M.; Rockenbauer, A.; Simaan, A. J.; Reglier, M. *Chem. Commun.* **2006**, 1027–1029.
(14) Judas, N.; Raos, N. *Inorg. Chem.* **2006**, *45*, 4892–4894.
(15) Ghattas, W.; Giorgi, M.; Gaudin, C.; Rockenbauer, A.; Réglier, M.; Simaan, A. J. *Bioinorg. Chem. Appl.* **2007**, 43424.

Computational Methods. Spin-restricted hybrid-DFT calculations were performed for the complexes [Cu(I)(ACC)(2,2′-bipyridine)] and [Cu(I)(ACC)(2,2′-bipyridine)(OOH)]$^-$, using Becke's three-parameter hybrid functional with the correlation functional of Lee, Yang, and Parr (B3LYP).[16,17] The LANL2DZ basis set was used for the calculations. It applies the Dunning/Huzinaga full double-ζ basis functions[18] on the first row and the Los Alamos effective core potentials plus DZ functions on all other atoms.[19] The suitability of B3LYP to predict structures and energetics is well-documented. All computational procedures were used as implemented in the Gaussian 03 package.[20] The optimizations were carried out using the Opt=Tight and Int=FineGrid options.

Activity Assays. *Activity assays on the Cu(II)−ACC complexes* were performed as follows: The complex (1 mM in 1 mL of methanol) was placed in the presence of 3 equiv of NaOH in a 16 mL hermetically sealed tube. Experiments were performed at 20 °C and under air, unless specified as being under nitrogen. Hydrogen peroxide (10 equiv) was then added through the septum to start the reaction. After 1 h, 0.5 mL of the headspace gas was removed using a gastight syringe, and ethylene production was quantified by gas chromatography. For the radical trap assays, experiments were carried out in the presence of 10 equiv of mannitol, benzoate, or methional.

Activity assays on the Cu(I)−ACC complexes were performed by mixing, in a dry box, 1 equiv of $Cu(CH_3CN)_4(PF_6)$ with 1 equiv of ACC and 1 equiv of the ligand in methanol to achieve a final concentration of 1 mM. A total of 1 mL of the resulting brown solution was placed in a 16 mL sealed tube with the additional desired amount of NaOH. 10 equiv of hydrogen peroxide were then added through the septum, and ethylene production was quantified after 1 h by gas chromatography, as described above for the Cu(II) complexes.

Gas chromatography measurements were performed on a CHROMPACK CP 9002 gas chromatograph equipped with a POROPAK Q 80/100 column (1/8″). The following conditions were used: vector = N_2, $T_{injector}$ = 150 °C, T_{oven} = 80 °C, $T_{detector}$ = 250 °C. Ethylene was quantified versus an external standard (Alltech 1% ethylene in nitrogen).

Physical Methods. *UV–visible spectra* were recorded on a VARIAN Cary 50 probe spectrometer. Low-temperature measurements were performed after adapting a HELLMA low-temperature probe (OT 0.5 or 1 cm) on the spectrophotometer. An ethanol/liquid N_2 bath was used to attempt the desired temperature. Alternatively, UV–vis spectra were recorded on a Hewlett-Packard 8453 photodiode array spectrophotometer equipped with a Unisoku thermostatted cell holder designed for low-temperature measurements (USP-203).

ESI-MS measurements were performed on a 3200 QTRAP spectrometer (Applied Biosystems SCIEX) equipped with a pneumatically assisted atmospheric pressure chemical ionization source. The ion spray voltage was 5500 V, and the orifice lens was 20 V. Alternatively, some ESI-MS spectra were acquired on a PE SCIEX API 2000 mass spectrometer.

EPR spectra were obtained using a BRUKER EMX9/2.7 spectrometer equipped with a B-VT2000 digital temperature controller (100–400 K). The simulations with automatic parameter fitting were performed for rhombic symmetry.[21] The contribution of naturally abundant ^{63}Cu and ^{65}Cu was considered, but the values given in the text refer to ^{63}Cu. All principal axes were supposed parallel. The line width anisotropy was described using the strain formula based on the local distribution of g and A_{Cu} tensors.

Electroanalytical experiments were performed with a CHI 660B electrochemical analyzer (CH Instruments), using a conventional three-electrode system. Cyclic voltammetry experiments were conducted at 0.1 V s^{-1} in a 15 mL three-compartment electrochemical cell equipped with an argon-purge system, at room temperature. Millimolar solutions of the complex were prepared in methanol with 0.1 M tetra-*n*-butylammonium perchlorate (TBAP) as a supporting electrolyte. The working electrode was a glassy carbon disk of 3 mm diameter. It was polished with 1 μm diamond paste prior to each recording. Potentials are referred to a standard Ag/AgCl, saturated KCl aqueous reference electrode. In these conditions, the redox potential of the regular ferrocenium/ferrocene redox couple was measured at 460 mV. The electrolyses were carried out using an EGG PAR model 173 potentiostat equipped with a model 179 digital coulometer. The glassy carbon electrode was replaced by a platinum plate electrode, and the UV–visible spectra were recorded during electrolysis using an optical HELLMA probe (OT = 1 cm) connected through optical fibers to a VARIAN CARY 50 spectrophotometer.

Results

Synthesis and Structural Characterization of Cu(II)−ACC and Cu(II)−AIB Complexes. The complexes were synthesized in methanol as previously described for **1a**.[13] Crystalline products were obtained by slowly evaporating concentrated methanol/water solutions. Crystallographic data for the different complexes are listed in Table 1.

The crystal structure of complex [Cu(2,2′-bipyridine)(ACC)(OH_2)](ClO_4) (**1a**) was described in our previous communication.[13] X-ray diffraction analysis was performed on a similar complex with AIB, [Cu(2,2′-bipyridine)(AIB)(OH_2)](ClO_4) (**1b**). AIB is a noncyclic analogue of ACC that cannot react to produce ethylene and that is known as an inhibitor of ACC oxidase activity.[22] The ORTEP drawings of the cations [Cu(2,2′-bipyridine)(ACC)(OH_2)]$^+$ and [Cu(2,2′-bipyridine)(AIB)(OH_2)]$^+$ are shown in Figure 1. The two structures are very similar, with the bipyridine ligand and the aminoacid moiety (ACC or AIB) forming the

(16) Becke, A. D. *J. Chem. Phys.* **1993**, *98*, 5648–5652.
(17) Lee, C.; Yang, W.; Parr, R. G. *Phys. Rev. B: Condens. Matter Mater. Phys.* **1988**, *37*, 785–789.
(18) Dunning, T. H., Jr.; Hay, P. J. *Modern Theoretical Chemistry*; Schaefer, H. F., III, Ed.; Plenum: New York, 1976.
(19) (a) Hay, P. J.; Wadt, W. R. *J. Chem. Phys.* **1985**, *82*, 270–283. (b) Hay, P. J.; Wadt, W. R. *J. Chem. Phys.* **1985**, *82*, 299–310. (c) Wadt, W. R.; Hay, P. J. *J. Chem. Phys.* **1985**, *82*, 284–298.
(20) Frisch, M. J.; Trucks, G. W.; Schlegel, H. B.; Scuseria, G. E.; Robb, M. A.; Cheeseman, J. R.; Montgomery, J. A., Jr.; Vreven, T.; Kudin, K. N.; Burant, J. C.; Millam, J. M.; Iyengar, S. S.; Tomasi, J.; Barone, V.; Mennucci, B.; Cossi, M.; Scalmani, G.; Rega, N.; Petersson, G. A.; Nakatsuji, H.; Hada, M.; Ehara, M.; Toyota, K.; Fukuda, R.; Hasegawa, J.; Ishida, M.; Nakajima, T.; Honda, Y.; Kitao, O.; Nakai, H.; Klene, M.; Li, X.; Knox, J. E.; Hratchian, H. P.; Cross, J. B.; Bakken, V.; Adamo, C.; Jaramillo, J.; Gomperts, R.; Stratmann, R. E.; Yazyev, O.; Austin, A. J.; Cammi, R.; Pomelli, C.; Ochterski, J. W.; Ayala, P. Y.; Morokuma, K.; Voth, G. A.; Salvador, P.; Dannenberg, J. J.; Zakrzewski, V. G.; Dapprich, S.; Daniels, A. D.; Strain, M. C.; Farkas, O.; Malick, D. K.; Rabuck, A. D.; Raghavachari, K.; Foresman, J. B.; Ortiz, J. V.; Cui, Q.; Baboul, A. G.; Clifford, S.; Cioslowski, J.; Stefanov, B. B.; Liu, G.; Liashenko, A.; Piskorz, P.; Komaromi, I.; Martin, R. L.; Fox, D. J.; Keith, T.; Al-Laham, M. A.; Peng, C. Y.; Nanayakkara, A.; Challacombe, M.; Gill, P. M. W.; Johnson, B.; Chen, W.; Wong, M. W.; Gonzalez, C.; Pople, J. A. *Gaussian 03*, revision B.03; Gaussian, Inc.: Wallingford, CT, 2004.
(21) Rockenbauer, A.; Korecz, L. *Appl. Magn. Reson.* **1996**, *10*, 29.
(22) Thrower, J.; Mirica, L. M.; McCusker, K. P.; Klinman, J. P. *Biochemistry* **2006**, *45* (43), 13108–13117.

Table 1. Crystallographic Data for the Complexes **2a**, **3a**, and **1b**

	2a	**3a**	**1b**
formula	$C_{16}H_{14}ClCuN_3O_6$	$C_{10}H_{14}ClCuN_3O_6$	$C_{14}H_{18}ClCuN_3O_7$
mw (g mol^{-1})	443.3	371.23	439.31
space group	$P2_1/c$	$P2_1/c$	$P2_1/c$
T (K)	293	293	243
λ (Å)	0.71073	0.71073	0.71073
D_{calcd} (g cm^{-3})	1.701	1.763	1.633
μ (cm^{-1})	14.67	17.84	14.14
a (Å)	12.4498(1)	9.7098(2)	11.340(4)
b (Å)	17.1635(4)	17.8062(5)	7.920(2)
c (Å)	8.5718(3)	8.6065(2)	22.197(6)
β (deg)	109.1061(9)	110.002(2)	116.326(6)
V (Å^3)	1730.74(7)	1398.26(6)	1786.8(9)
Z	4	4	4
R [$F^2 > 4\sigma F^2$]	0.0456	0.0467	0.0657
wR[a]	0.1261	0.1068	0.1694

[a] $w = 1/[\sigma^2(Fo^2) + (xP)^2 + yP]$ where $P = (Fo^2 + 2Fc^2)/3$]. **2a**: $x = 0.0624$, $y = 1.0025$. **3a**: $x = 0.0358$, $y = 3.2244$. **1b**: $x = 0.0824$, $y = 0.5896$.

basal plane around the Cu(II) ion in a square-pyramidal geometry. A water molecule occupies the axial position. In each structure, the amino acid is coordinated in a bidentate mode *via* the nitrogen and one oxygen, as suggested for the enzyme–substrate complex at the first stage of the catalytic mechanism.[7,8] A survey of the Cambridge Structural Database revealed that this coordination is similar to that found in previously characterized copper(II)−amino acid complexes.[23]

X-ray diffraction analysis was also performed on complexes **2a** and **3a**. The ORTEP drawings are shown in Figure 2. The copper(II) ions are in square-pyramidal geometries, and the overall structures are very similar to those obtained with the bipyridine ligand. However, in **2a** and **3a**, the axial position on the Cu(II) ion is occupied by the second oxygen atom from the carboxylate function of an ACC coming from a neighboring entity, whereas in **1a** and **1b**, this position is occupied by a water molecule. Therefore, **2a** and **3a** form chains in the solid state. These chains probably fall apart in solution, producing the aqua or methanol bound monomers, as indicated by the solution studies described below.

Selected bond lengths and angles for the four complexes as well as the structural indices τ are presented in Table 2. Structural indices were calculated as described by Addison et al.[24] for five-coordinate structures. It measures the degree of trigonality ($\tau = 0$ for a perfect square-based pyramid geometry and $\tau = 1$ for perfectly trigonal bipyramidal geometry). For the four complexes, τ ranged from 0.07 to 0.11, indicating small deviation from perfectly square-pyramidal geometry. The Cu(II)−ACC(AIB) distances, Cu1−N1 and Cu1−O2, range from 1.993 to 2.005 Å and 1.916 to 1.9557 Å, respectively. These bond lengths are in good agreement with the average distances of Cu(II)−amino acid complexes found in the Cambridge Structural Database (ranging from 1.96 to 2.03 Å for Cu−N and from 1.91 to 1.97 Å for Cu−O bonds).[23] The exogenous ligand is coordinated to the copper ion at distances of Cu−N ranging from 1.985 to 2.026 Å. The oxygen atom on the elongated axial position (from water in the cases of **1a** and **1b** and from ACC in the cases of **2a** and **3a**) stands at distances between 2.23 and 2.42 Å. Finally, as we already observed for complex **1a**,[13] within the ACC moiety, the C3−C4 distance is shorter than the similar distance in a free ACC molecule for which several X-ray structures have been obtained.[25,26] Indeed, coordinated ACC displays a C3−C4 distance varying here from 1.469 to 1.483 Å, whereas the length for the same bond ranges from 1.490 to 1.497 Å in unbound ACC. A similar shortening is observable in complexes with ACC pyridoxal Schiff-base ligated to Cu(II) or Ni(II) ion.[27,28] This shortening is accompanied by a slight closure of the C3−C2−C4 angle (found at values ranging from 58.9 to 59.2° in complexes **1a** to **3a**, versus values ranging from 59.6 to 59.8 in unbound ACC).

Characterization in Solution. The UV–visible spectra were recorded in methanol, and the different complexes present characteristic d−d transitions around 600 nm ($\epsilon \sim 100$ mol^{-1} L cm^{-1}).

Methanolic solutions of complexes **1a**, **1b**, **2a**, and **3a** were analyzed by electrospray ionization mass spectrometry in the positive mode. For **1a** and **1b**, the spectra exhibited major peaks with characteristic isotopic patterns at $m/z = 318.8$ and $m/z = 320.9$, respectively. These peaks are attributed to the cations [Cu(2,2′-bipyridine)(ACC)]$^+$ and [Cu(2,2′-bipyridine)(AIB)]$^+$, respectively, without the coordinated water molecule. For **2a** and **3a**, the spectra revealed major peaks with characteristic isotopic patterns at $m/z = 343.0$ and $m/z = 271.0$, respectively. They are attributed to the cations [Cu(1,10-phenanthroline)(ACC)]$^+$ and [Cu(2-picolylamine-)(ACC)]$^+$, respectively, indicating that the polymeric chains, observed in the solid state structures, probably dissociated to give rise to monomers in solution.

The X-band EPR spectra of the complexes were recorded at 120 K in frozen MeOH solutions (see the Supporting Information). They were all found to be very similar. They are characteristic of Cu(II) ions in a square-planar derived geometry in accordance with the solid state structures, and they also support the indication that **2a** and **3a** probably dissociate in solution to give independent monomers. Good simulations required the use of rhombic symmetry. The EPR constants obtained from the simulation are reported in Table 3.

The z direction can be evidently assigned to the axis perpendicular to the plane of the square-pyramidal structure, since in this direction both the copper hyperfine structure and g are large. As concerning the assignment of x and y directions, the nitrogen superhyperfine structure may offer information. For these lines in the perpendicular domain of the spectra, a good fit was obtained if we assumed two distinct superhyperfine tensors. Among them, two nitrogen tensors were equivalent, and the third was different. Though the resolution was excellent in the case of **1b**, even in this

(23) Allen, F. H. *Acta Crystallogr., Sect. B* **2002**, *58*, 380.
(24) Addison, A. W.; Rao, T. N.; Reedijk, J.; van Rijn, J.; Verschoor, G. C. *J. Chem. Soc., Dalton Trans.* **1984**, 1349–1356.
(25) Pirrung, M. C. *J. Org. Chem.* **1987**, *52* (19), 4179–4184.
(26) Valle, G.; Crisma, M.; Toniolo, C.; Holt, E. M.; Tamura, M.; Bland, J.; Stammer, C. H. *Int. J. Pept. Protein Res.* **1989**, *34*, 56.
(27) Aoki, K.; Yamazaki, H. *J. Chem. Soc., Chem. Commun.* **1987**, 1241–1242.
(28) Aoki, K.; Hu, N.; Yamazaki, H. *Inorg. Chim. Acta* **1991**, *186* (2), 253–261.

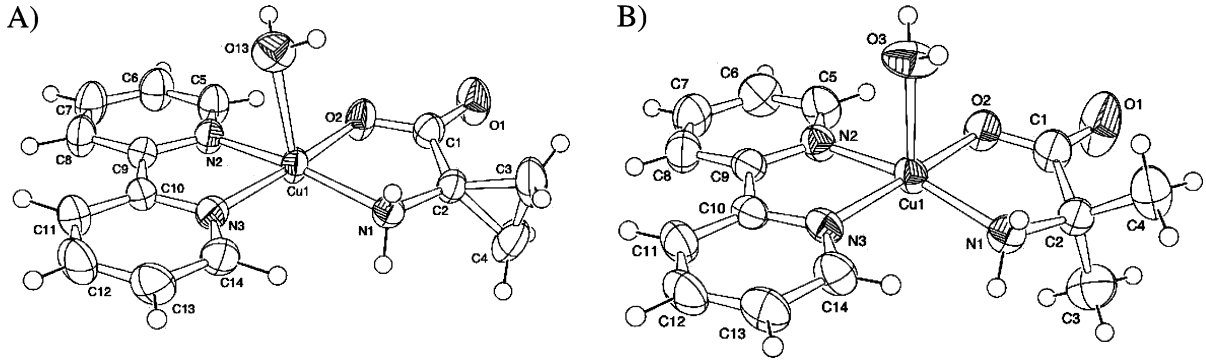

Figure 1. ORTEP drawings of the cations (A) [Cu(2,2′-bipyridine)(ACC)(OH_2)]$^+$ (cation of **1a**) and (B) [Cu(2,2′-bipyridine)(AIB)(OH_2)]$^+$ (cation of **1b**).

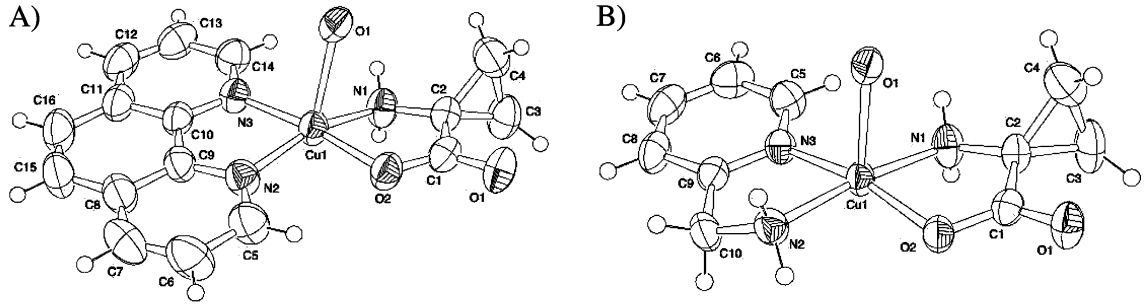

Figure 2. ORTEP drawings of the cations (A) [Cu(1,10-phenanthroline)(ACC)]$^+$ (cation of **2a**) and (B) [Cu(2-picolylamine)(ACC)]$^+$ (cation of **3a**).

Table 2. Selected Bond Lengths, Bond Angles, and Structural Indices (τ)[24] for [Cu(2,2′-bipyridine)(ACC)(H_2O)]$^+$ **1a**, [Cu(2,2′-bipyridine)(AIB)(H_2O)]$^+$ **1b**, [Cu(1,10-phenanthroline)(ACC)]$^+$ **2a**, and [Cu(2-picolylamine)(ACC)]$^+$ **3a**

	1a	**1b**	**2a**	**3a**
		Bond Lengths (Å)		
Cu1−O2	1.916(2)	1.937(2)	1.9389(18)	1.9557(3)
Cu1−N1	2.005(2)	1.987(2)	1.999(2)	1.993(4)
Cu1−N2	1.985(3)	1.997(2)	1.999(2)	1.996(4)
Cu1−N3	2.011(3)	2.017(2)	2.026(2)	2.011(3)
Cu1−O_{axial}	2.421(3)	2.292(2)	2.237(2)	2.232(3)
C3−C4	1.483(6)		1.482(5)	1.469(9)
		Bond Angles (deg)		
O2−Cu1−N1	84.92(9)	84.56(8)	84.22(9)	84.09(14)
N1−Cu1−N3	100.51(10)	98.95(9)	100.60(9)	99.59(15)
N3−Cu1−N2	81.52(10)	81.17(9)	82.05(9)	83.02(15)
N2−Cu1−O2	93.00(10)	94.66(8)	91.70(9)	92.07(13)
O2−Cu1−O_{axial}	95.73(10)	92.61(10)	94.08(8)	95.55(12)
C3−C2−C4	59.2(3)	111.1(3)	59.2(2)	58.9(4)
		Structural Index		
τ	0.08	0.07	0.11	0.07

Table 3. EPR Constants for **1b**, **1a**, **2a**, and **3a** in MeOH Obtained from the Simulation[a]

	1b	**1a**	**2a**	**3a**
g_x	2.057	2.064	2.060	2.061
A_{Cu}	19.6	22.2	17.9	15.4
$A_{N(2)}$	12.4	11.8	10.6	13.2
$A_{N(1)}$	10.8	9.6	13.3	12.6
g_y	2.044	2.039	2.049	2.042
A_{Cu}	22.5	21.9	21.7	18.8
$A_{N(2)}$	9.7	6.1	6.7	6.1
$A_{N(1)}$	12.0	10.7	11.1	9.9
g_z	2.237	2.235	2.245	2.236
A_{Cu}	180.4	181.0	177.0	185.5
$A_{N(2)}$	10.6	12.4	7.1	10.9
$A_{N(1)}$	7.0	8.5	12.6	3.6

[a] Coupling constants are expressed in 10^{-4} T. The contribution of naturally abundant ^{63}Cu and ^{65}Cu is considered, but here the values refer to ^{63}Cu.

case, unique parameter determination was not possible if we adjusted three different nitrogen tensors due to the large number of independent fitting parameters. The assignment of nitrogen tensors still has some uncertainty. The molecular structure would suggest that the two equivalent $A_{N(2)}$ tensors can be assigned to the N2 and N3 nitrogens of the exogenous ligand, and $A_{N(1)}$ can be assigned to the nitrogen of the ACC ligand. It contradicts, however, the anisotropy of nitrogen tensors, since always the largest principal value is expected in the bond direction between the nitrogen and the copper. In the *x* direction, we always found a larger $A_{N(2)}$ than in the *y* direction, while for $A_{N(1)}$—at least in the cases where the good resolution offers a better confidence (**1b** and **1a**)—the *y* direction renders the larger value. Thus, probably, the *x* direction corresponds to the N1−Cu1−N2 bonds and the *y* direction to the closely orthogonal N3−Cu1 bond in Figure 1.

Redox Properties. The electrochemical properties of copper(II)−ACC complexes were studied by cyclic voltammetry (CV) in methanol, at room temperature and under argon. The CV curves are displayed in Figure 3, and the characteristic potentials (vs Ag/AgCl saturated KCl aqueous reference electrode) are reported in Table 4.

While scanning toward the negative range of potentials, the CV curves are characterized by one reduction peak attributed to the cathodic reduction of Cu(II) into Cu(I) at –168, –200, and –432 mV for complexes **2a**, **1a**, and **3a**, respectively. For **3a**, this system is partially overlapped by a second one corresponding to the deposition of Cu(0) onto the electrode surface as revealed on the CV curve by a sharp and intense redissolution peak at +210 mV on the reverse scan, in addition to extra unassigned anodic peaks probably

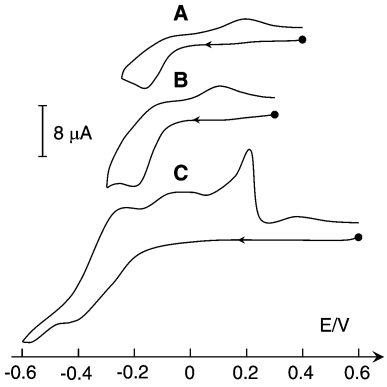

Figure 3. CV curves of 1 mM solutions of Cu(II)−ACC complexes in methanol + 0.1 M TBAP. $\upsilon = 0.1$ V s^{-1}. Potentials vs Ag/AgCl. WE: GC ($f = 3$ mm). (A) [Cu(1,10-phenanthroline)(ACC)](ClO$_4$) (**2a**). (B) [Cu(2,2′-bipyridine)(ACC)](ClO$_4$) (**1a**). (C) [Cu(picolylamine)(ACC)](ClO$_4$) (**3a**). Apparent $E_{1/2} = 15$ mV and –48 mV for **2a** and **1a**, respectively.

Table 4. Redox Characteristics of the Cu(II)−ACC Complexes and Ethylene Yields[a]

	redox characteristics (vs AgCl/Ag)		ACC conversion into ethylene (%)	
complex	E_{red} (mV)	E_{ox} (mV)	under air	under N_2
1a	−200	104	67	97
2a	−168	198	70	100
3a	−432	−35	33	43

[a] 1 mM solution in methanol, 3 equiv of NaOH, 10 equiv H_2O_2 after 1 h.

due to the demetalation of the complex. For all of the complexes, the first one-electron signal does not appear fully reversible; the differences between reduction and oxidation peaks are much higher than the expected 60 mV for a fully reversible one-electron process. Accordingly, on the reverse scan, the corresponding reoxidation peaks are seen at +198, +104, and –35 mV for **2a**, **1a**, and **3a**, respectively. This indicates that a chemical reaction is coupled with the electron transfer leading to the nonreversibility. This change does not lead to a decomposition of the complexes since several cycles can be performed without altering the cathodic and anodic waves. It corresponds to reversible changes in the coordination sphere around the copper center; that is, the electron transfer is accompanied by a geometric change in the structure of the complex to achieve its stabilization, likely from square-planar in the Cu(II) state to tetrahedral in the Cu(I) state. This hypothesis has been confirmed by DFT calculations (see below). In addition, it appears that, as expected, the stability of the Cu(I) redox state increases with the π-accepting capability of the exogenous ligand: **2a** > **1a** > **3a**.

Ethylene Production by the Cu(II)−ACC Complexes. Under Air. Ethylene production was measured by gas chromatography after 1 h. The reaction was performed by adding 3 equiv of base and various equivalents of hydrogen peroxide to methanolic solutions of the different copper−ACC complexes (1 mM). The maximum yield was achieved using a minimum of 8–10 equiv of H_2O_2. Therefore, all of the following experiments were carried out using 10 equiv of hydrogen peroxide. The results are reported in Table 4. Under air, complexes **1a** and **2a** react with H_2O_2 to release ethylene with a yield of *ca*. 70%, whereas complex **3a** is less reactive, and only 33% of ACC is oxidized into ethylene. In order to compare with the ethylene production performed by free copper ions, a 1 mM solution of Cu(ClO$_4$)$_2$·6H$_2$O in the presence of 1 equiv of ACC was prepared. Ethylene production was investigated under the same conditions, and the yield hardly reached 15%. This is roughly 2−5 times lower than with complexes **1a** to **3a**, and these results underline that the presence of an exogenous ligand is important for the reactivity. It was verified that uncoordinated ACC is not oxidized in significant quantity under the same experimental conditions.

Under Nitrogen. The reactions were also performed in the absence of dioxygen (see Table 4) and with various equivalents of hydrogen peroxide. The dependence upon the amount of hydrogen peroxide used was identical under air and under nitrogen. Under an inert atmosphere and using 10 equiv of hydrogen peroxide, ethylene production with complexes **1a** and **2a** was quantitative, and it reached 43% (vs 33% under air) with complex **3a**. This showed that dioxygen is not necessary for the oxidation of ACC. In fact, it rather appeared that O_2 has a negative influence on the reactivity since the conversion yields were higher without dioxygen.

In the Presence of ROS Scavengers. In order to provide more insights into the nature of the oxidizing species responsible for the oxidation of ACC into ethylene (hydroxyl radical, hydroperoxyl radical, or metal-controlled oxidant), the reactivity assays were performed in the presence of various ROS scavengers. The reactions were first carried out in the presence of 10 mM of a hydroxyl radical scavenger, mannitol.[29] No change in ethylene production was observed. Considering the reaction being held in methanol, which is also a hydroxyl radical scavenger, it is reasonable to think that the oxidation of ACC into ethylene is not mainly due to free hydroxyl radicals. The presence of a hydroperoxyl radical scavenger, methional, did not affect the conversion yield either. We can hence conclude that the oxidation of ACC into ethylene by the copper(II) complexes implies a metal-centered oxidizing species.

Characterization of a Brown Intermediate. In the Presence of Hydrogen Peroxide. The complexes display a weak absorption band at around 600 nm. The addition of 3 equiv of NaOH did not affect their UV–visible spectra. When complexes **1a** and **2a** were treated with H_2O_2 at a low temperature (−20 °C), a surprising color change occurred and the solutions became dark brown. In the case of **3a**, this species could not be detected. The brown intermediates are characterized by a strong absorption centered at 433 and 440 nm for **1a** and **2a**, respectively, with $\epsilon = 2200$–2300 M^{-1} cm^{-1}, as determined by spectroelectrochemistry experiments. These species decomposed rapidly (within a few minutes at –20 °C), and the solution turned green. When the experiments were carried out under an inert atmosphere, two isosbestic points were observed during the decomposition of the brown species (see Figure 4A for complex **1a**). This is in accordance

(29) Schweigert, N.; Acero, J. L.; von Gunten, U.; Canonica, S.; Zehnder, A. J. B.; Eggen, R. I. L. *Environ. Mol. Mutagen.* **2000**, *36*, 5–12.

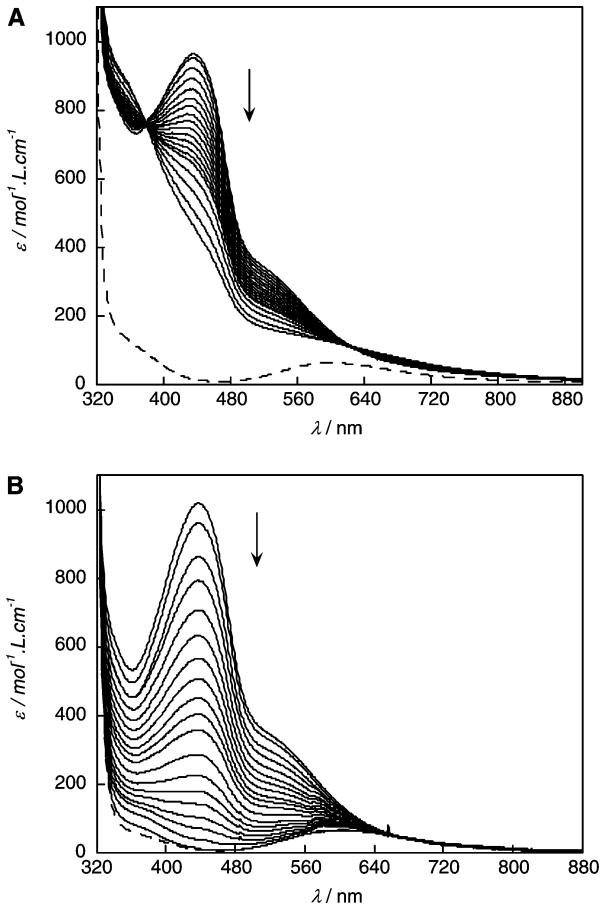

Figure 4. UV–visible detection of the brown intermediate in methanol and its decomposition with time from a 1 mM methanolic solution of complex [Cu(2,2′-bipyridine)(ACC)](ClO_4) (**1a**): (A) under nitrogen, with 3 equiv of base at –20 °C, before (---) and after (——) addition of 10 equiv of hydrogen peroxide over 360 s, and (B) at 20 °C under air, before (---) and after (——) addition of 1 equiv of ascorbate over 1500 s.

with the quantitative yield of ethylene production previously described under nitrogen.

Similar intermediates were formed with the copper(II)−AIB complexes. When **1b** was treated, at room temperature, with an excess of hydrogen peroxide in the presence of a base, the brown intermediate was formed and could be monitored by UV–visible spectroscopy. The intermediate displayed an absorption band at 435 nm, similar to the one obtained with **1a**. It decayed to give back the initial complex with only a small amount of decomposition. The experiment could be reproduced several times without leading to notable deterioration of **1b**.

EPR Characterization. The increase and decay of the UV–visible band at 440 nm was followed as a function of time in the case of complex **2a**, [Cu(1,10-phenanthroline)(ACC)](ClO_4), which provides the most stable intermediate (see Figure 5). Experiments were performed under air, at room temperature, and during the course of the reaction, several aliquots were sampled at known times and quickly frozen in liquid nitrogen. X-band EPR spectra were then recorded at 120 K on these aliquots (Figure 5A). The initial spectrum of complex **2a** was recorded before the addition of H_2O_2 and in the presence of 3 equiv of the base. Then, 15 s after the addition of hydrogen peroxide, the EPR

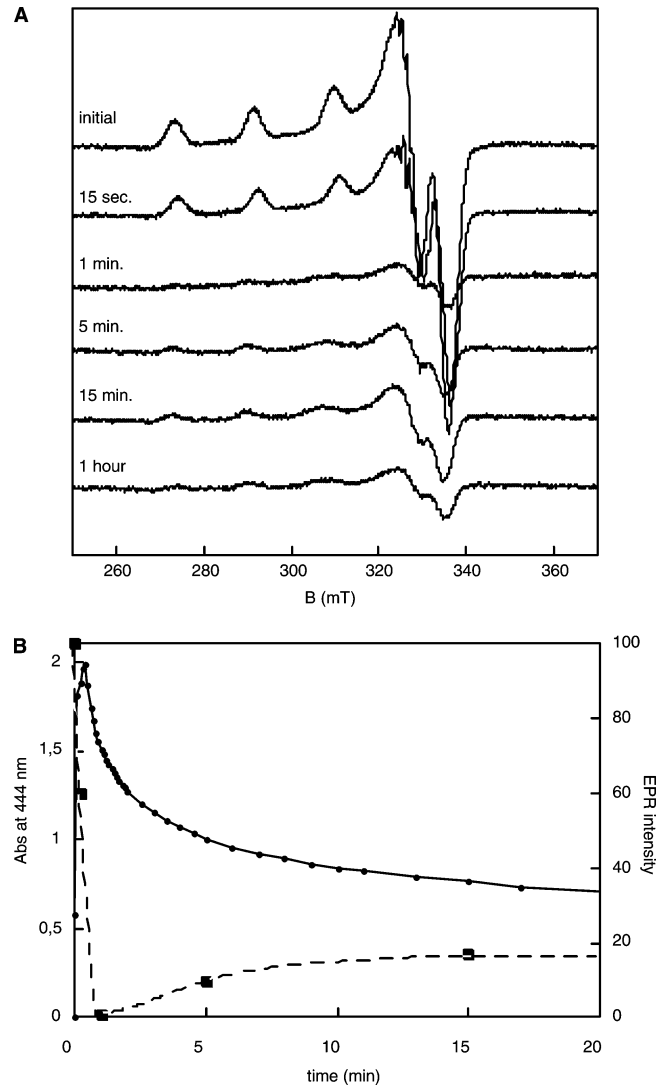

Figure 5. (A) X-band EPR spectra during the course of formation and decay of the brown intermediate generated with complex **2a** (1 mM) in methanol, under air and at 20 °C (10 equiv of H_2O_2, 3 equiv of NaOH). EPR conditions: 120 K; microwave power, 20 mW; modulation frequency, 100 kHz; modulation amplitude, 2 G. (B) EPR intensity relative to the initial intensity and absorbance at 440 nm as a function of the reaction time after addition of hydrogen peroxide on a 1 mM solution of **2a**. EPR intensities were estimated by double integration of the derivative signal.

spectrum was found to be similar to the one of **2a** but with lower intensity (roughly 50% of the initial intensity). After 1 min, the EPR spectrum was almost silent, and only a weak signal from the initial complex remained. At the same time, the UV–vis band was at a maximum (Figure 5B). These results indicate that the brown intermediate is EPR-silent. Then, the signal from the initial complex reappeared, and at the end of the reaction, 17% of the initial intensity was recovered. Hence, more than 80% of the final species were composed of EPR-silent species, probably dimeric or polymeric copper(II) species.

A small part of the complex that did not react was thus regenerated in its initial form (roughly 17%). These observations were confirmed by ESI-MS (positive mode) experiments that were performed on complex **1a**. The brown intermediate could not be identified using this technique. Nevertheless, at the end of the reaction, the presence of the

m/z = 318.8 peak attributed to the [(2,2′-bipyridine)-Cu(ACC)]$^+$ cation clearly indicated partial regeneration of the initial complex.

Monocrystals were obtained from the resulting solution after the reaction of **1a** with hydrogen peroxide. The structure of complex **1af** was determined by X-ray diffraction analysis (see the Supporting Information). It reveals a polymeric assembly of copper(II), carbonates, and sodium ions with a raw formula of $Cu(CO_3)_2Na_2 \cdot 3H_2O$ that certainly represents only a part of the decomposition products.

Effect of Ascorbate. The addition of ascorbate on a methanolic solution of the copper(II)−ACC complexes (**1a** and **2a**) produced the same intermediate (see Figure 4B in the case of complex **1a**). This brown species decomposed to give the initial Cu(II)−ACC complex back, as indicated by the UV–visible spectrum. No ethylene was produced using these experimental conditions. Finally and surprisingly, the intermediate could also be formed using ascorbate under an inert atmosphere, and it was found to be stable in the absence of dioxygen.

This leads to the conclusion that the brown intermediate is probably a "Cu(I)−ACC" complex, in agreement with the absence of an EPR signal, as described above. The 440 nm transition can thus be attributed to a metal-to-ligand charge-transfer transition from the 3d orbital of the Cu(I) toward a low-lying π^* of the pyridine ligands, as assigned by Irving and Williams for [Cu^I(NN)$_2$]$^+$ complexes.[30] The differences in stability of the Cu(I)−ACC species can be correlated to the reduction and oxidation potentials of complexes **1a** to **3a**. Indeed, with the phenanthroline ligand, the Cu(I) state was more stable. With the bipyridine ligand, the stability was slightly lower, and finally, in the case of the picolylamine, the Cu(I) state could not be detected.

Spectroelectrochemistry. In order to unambiguously demonstrate the Cu(I) redox state of the intermediate, we have performed spectroelectrochemical experiments with the complex [Cu(2,2′-bipyridine)(ACC)(H$_2$O)](ClO$_4$) (**1a**). Electrolysis was carried out at room temperature, under argon, and at –300 mV versus Ag/AgCl. The electronic spectra were recorded during the course of the reduction process using an optical fiber. The results are presented in Figure 6. The reduction of the Cu(II) complex is accompanied by an increase of the 433 nm ligand-to-metal charge transfer transition. The maximal intensity of the band is reached after *ca.* 1.9 carbons have been consumed, which corresponds to 1 equiv of electron per complex. This confirms, together with the absence of an EPR signal, as previously observed, that the observed brown species is [Cu^I(2,2′-bipyridine)(ACC)]. We thus propose that the brown intermediates detected during the course of the reaction with hydrogen peroxide are Cu(I)−ACC or Cu(I)−AIB complexes generated by reduction of the corresponding Cu(II) complexes. This reduction is probably performed by the deprotonated form of hydrogen peroxide, known as being more reductant than the protonated one.[31] The role of the base would thus be to generate HOO$^-$,

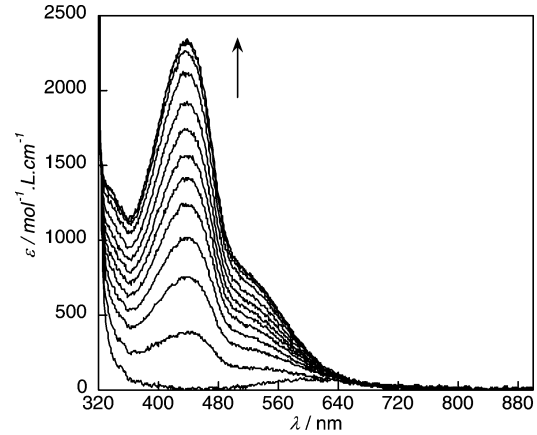

Figure 6. UV–vis spectra recorded during the exhaustive potentiostatic electrolysis at –0.3 V of a 0.5 mM methanol solution of complex [Cu(2,2′-bipyridine)(ACC)(H$_2$O)]ClO$_4$ (**1a**).

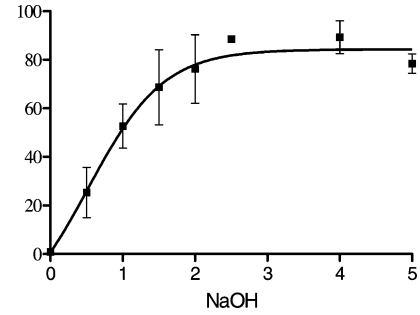

Figure 7. Ethylene production (after 1 h) as a function of the base added for a 1 mM methanolic solution of [Cu(I)(CH$_3$CN)$_4$]·PF$_6$, ACC, and 1,10-phenanthroline, in the presence of 10 equiv of hydrogen peroxide.

as already proposed,[13] in order to allow the reduction of Cu(II) ions.

Reactivity Studies of the Cu(I)−ACC Complexes. The Cu(I)−ACC complexes could not be isolated in the solid state. They were thus prepared in the glovebox by mixing in methanol, the desired exogenous ligand (2,2′-bipyridine or 1,10-phenanthroline) with [Cu(I)(CH$_3$CN)$_4$](PF$_6$), and ACC. The formation of the brown Cu(I) complex was monitored in UV–visible spectroscopy, and it required the addition of at least 1 equiv of base (probably for ACC deprotonation) to reach the maximum intensity of the band around 435 nm.

The mixture of Cu(I) with the exogenous ligand and ACC was directly used for the activity assays at a concentration of 10^{-3} M. The conversion yield of ACC into ethylene, with 10 equiv of hydrogen peroxide, under these conditions is presented as a function of the equivalents of base added in Figure 7, where phenanthroline was used as the exogenous ligand. The experiments were repeated up to seven times for each point to get better reliability.

When no NaOH was added, less than 1% of the ACC was converted into ethylene. When 1 equiv of NaOH was added, the ACC was deprotonated, and the Cu(I)−ACC complex was almost quantitatively formed on the basis of the UV–visible analysis. Under these conditions, the yield of ethylene production was ca. 50%. The maximum of ethylene

(30) Irving, H.; Williams, R. J. P. *J. Chem. Soc.* **1953**, 3192–3210.

(31) Sawyer, D. *Oxygen Chemistry; International Series of Monographs on Chemistry, 26*; Oxford University Press; New York, 1991.

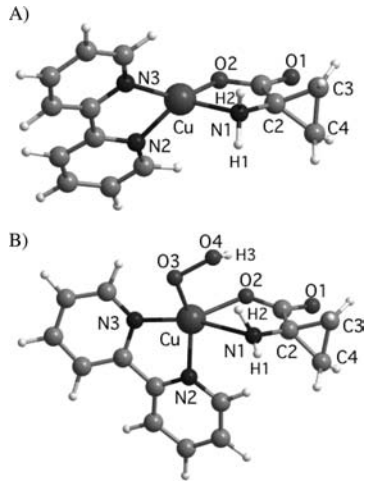

Figure 8. Optimized structures of (A) [Cu(I)(2,2′-bipyridine)(ACC)] and (B) [Cu(I)(2,2′-bipyridine)(ACC)(OOH)]$^-$.

production required at least 1.5 to 2 equiv of base, and it reached roughly 85%. Under the same conditions, the corresponding Cu(II)−ACC complex, **2a**, was able to quantitatively convert the bound ACC moiety into ethylene (see Table 4). The conversion yields here are probably slightly lowered by the fact that the complex could not be isolated and was prepared *in situ*. A second equivalent of base was thus necessary to reach the maximum of ethylene production. It is probably involved in hydrogen peroxide deprotonation to provide HOO^-. The latter may have stronger nucleophilicity than the protonated form and may be able to coordinate on the Cu(I) ion to generate a Cu(I)−OOH species following a Fenton-like reaction.[32,33]

DFT Calculations. In order to investigate possible structures of [Cu(I)(2,2′-bipyridine)ACC] and its "HOO" adduct, DFT calculations have been performed (Figure 8). Selected bond lengths and angles for the geometry-optimized complexes are listed in Table 5.

The initial geometry was taken from the crystal structure of [Cu(II)(2,2′-bipyridine)(ACC)(OH_2)]$^+$ with a square-planar CuN_3O structure, but the optimized structure of [Cu(I)(2,2′-bipyridine)ACC] reveals a distorted tetrahedral N_3O coordination around the copper, which is in reasonable agreement with the tetrahedral preference of copper(I). It is also in agreement with the crystallographic structures of several Cu(I) complexes with a 2,2′-bipyridine ligand such as [Cu(I)(2,2′-bipyridine$)_2$]$^+$, for instance.[34] This geometric change between the copper(II) and copper(I) redox state could be responsible for the nonreversibility of the redox process, as observed during the electrochemistry experiments.

On the other hand, the computed structure of the Cu(I)−hydroperoxo species exhibits a distorted trigonal-bipyramidal structure. The short O4−H2 (1.97 Å) and O2−H3 (2.11 Å) distances indicate the formation of a hydrogen-bonding network. These hydrogen-bonding interactions make the two N−H bonds nonequivalent (i.e., N1−H1 = 1.017 Å vs N1−H2 = 1.029 Å). This contrasts with the [Cu(I)(2,2′-bipyridine)ACC] complex where the two N−H bonds were found to have the same length of 1.021 Å.

Table 5. Selected Bond Lengths and Bond Angles for the Optimized Structures of [Cu(I)(2,2′-bipyridine)(ACC)] and Its Hydroperoxo Adduct [Cu(I)(2,2′-bipyridine)(ACC)(OOH)]$^-$

	[Cu(I)(2,2′-bipyridine)(ACC)]	[Cu(I)(2,2′-bipyridine)(ACC)(OOH)]$^-$
	Bond Lengths (Å)	
Cu−O2	1.993	2.069
Cu−N1	2.144	2.855
Cu−N2	2.100	2.043
Cu−N3	2.037	2.080
Cu−O3		1.993
O3−O4		1.529
C3−C4	1.525	1.535
	Bond Angles (deg)	
O2−Cu−N1	84.3	65.8
N1−Cu−N3	120.4	159.2
N3−Cu−N2	80.3	79.5
N2−Cu−O2	120.4	134.94
O2−Cu−O3		98.9
C3−C2−C4	59.6	59.8

Discussion and Conclusion

Possible Mechanism. We have thus identified the brown intermediate of the Cu(II)−ACC/H_2O_2 reaction to be the neutral Cu(I)−ACC complex. The reaction first proceeds *via* a reduction step, and the optimized DFT structure of the Cu(I)−ACC intermediate (with the bipyridine ligand) reveals a change in geometry: the square-planar Cu(II)−ACC complexes are thus reduced in tetrahedral Cu(I)−ACC complexes. These reduced species are generated when the Cu(II) complexes are treated with hydrogen peroxide in a basic medium. The base is involved in the deprotonation of H_2O_2, leading to HOO^-, a more powerful reductant[31] that is capable of reducing the Cu(II) ions. Similar brown species have also been described by Pattubala et al. with several ternary Cu(II) complexes, with 2,2′-bipyridine and α-amino acid salicylaldiminates, effective in benzylamine oxidation.[35] During the course of the reaction of the complexes with hydrogen peroxide, the authors have observed an initial light-brown solution that does not show any d−d band in UV–visible spectroscopy. In light of our results, these brown species most likely correspond to Cu(I) forms of the initial complexes. Furthermore, the ability of hydrogen peroxide to reduce Cu(II) complexes has also been mentioned by the group of Itoh, using the ligand tris[2-(2-pyridyl)ethyl]amine, TEPA.[36] The authors have indeed described the formation of the Cu(II)−hydroperoxo intermediate supported by the ligand TEPA, which was then converted into the correspond-

(32) Fenton, H. J. H. *J. Chem. Soc.* **1894**, *65*, 899.
(33) (a) Sawyer, D. T.; Sobkowiak, A.; Matsushita, T. *Acc. Chem. Res.* **1996**, *29*, 409–416. (b) Sawyer, D. T. *Coord. Chem. Rev.* **1997**, *165*, 297–313.
(34) (a) Foley, J.; Tyagi, S.; Hathaway, B. J. *J. Chem. Soc., Dalton Trans.* **1984**, 1–5. (b) Munakata, M.; Kitagawa, S.; Asahara, A.; Masuda, H. *Bull. Chem. Soc. Jpn.* **1987**, *60*, 1927–1929. (c) Skelton, B. W.; Waters, A. F.; White, A. M. *Aust. J. Chem.* **1991**, *44*, 1207–1215. (d) Tomislav, P. *Acta Crystallogr., Sect. E* **2006**, *62*, 3.
(35) Pattubala, A. N. R.; Munirathinam, N.; Chakravarty, A. R. *Inorg. Chim. Acta* **2002**, *337*, 450–458.
(36) Osako, T.; Nagatomo, S.; Tachi, Y.; Kitagawa, T.; Itoh, S. *Angew. Chem., Int. Ed.* **2002**, *41*, 4325–4328.

Scheme 2. Possible Mechanism and Proposed Intermediates for the Oxidation of ACC into Ethylene with Hydrogen Peroxide by Cu(II) Complexes

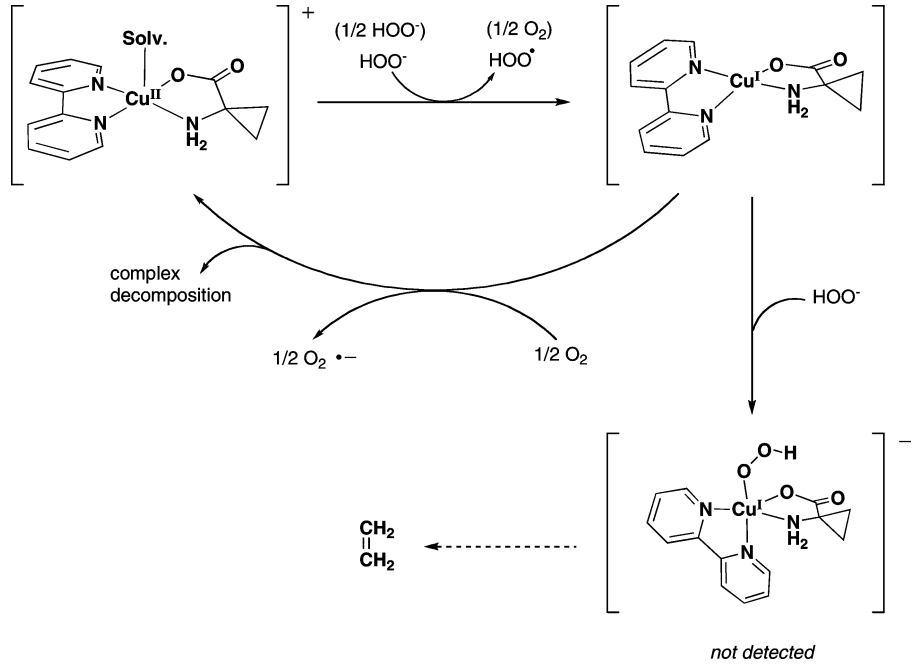

ing $[Cu^{I}(TEPA)]^{+}$ complex. Even though they did not describe it in detail, the tetradentate ligand TEPA greatly stabilizes the Cu(I) state, and the Cu(I) complex does not show reactivity toward dioxygen.[37] In our case, the exact mechanism of reduction of the Cu(II)−ACC complexes into Cu(I)−ACC by hydrogen peroxide is not clear, but it could proceed *via* the formation of an undetectable Cu(II)−OOH intermediate, as described by Itoh and collaborators.[36]

The Cu(I)−ACC intermediates can be prepared *in situ* by mixing the Cu(I) salt with the ligand and deprotonated ACC, or alternatively by reduction of the Cu(II)−ACC complexes with ascorbate. These copper(I) species do not react with O_2 to produce ethylene. Hydrogen peroxide is necessary for the oxidation of ACC into ethylene. Instead, they are reoxidized into Cu(II) by O_2, as seen in Figure 4B. This leads to a lower yield of ethylene production under air as compared to the experiments under nitrogen (see Table 4). Moreover, we observed that the reaction of Cu(I)−ACC complexes with H_2O_2 to produce ethylene probably requires the deprotonation of hydrogen peroxide since 2 equiv of NaOH are needed to reach the maximum conversion yield: one is involved in ACC deprotonation to favor its coordination on the metal ion, the second one would thus generate HOO^{-}, more nucleophilic than H_2O_2. We thus propose that the Cu(I) complexes react with hydrogen peroxide to generate Cu(I)−OOH species following a Fenton-type chemistry.[32] Such intermediates have already been proposed in the case of oxidative DNA degradation with copper ions[38,39] but have never been characterized to date.

The question now concerns the following step of the reaction and the nature of the oxidizing species. In the case of oxidative DNA degradation with copper ions, studies with ROS scavengers have led to the conclusion that hydroxyl radicals were not the main oxidants causing DNA damage.[39,40] Moreover, several studies on the reaction of H_2O_2 with Cu(I) complexes have indicated that free hydroxyl radicals were probably not formed.[41] Yet, the reaction of metal ions with hydrogen peroxide is very controversial.[33,42] In our case, when the reaction is carried out in the presence of radical scavengers such as mannitol or methional, the yield of ethylene production is unchanged. This is in favor of a metal-centered oxidizing species, although additional experimental data are needed to get more insight into the mechanism of ACC oxidation by the Cu(II)−ACC complexes.

A possible mechanism is summarized in Scheme 2.

Cu(I)−OOH versus Cu(II)−OOH. We have isolated several copper(II)-ACC complexes that have been characterized by X-Ray diffraction analysis, as well as a copper(II)-AIB complex. These Cu(II)-ACC complexes are able to convert the bound ACC into ethylene in the presence of hydrogen peroxide and a few equivalents of base. The reaction first proceeds *via* the reduction of the square-planar Cu(II)-ACC complexes in tetrahedral Cu(I)-ACC complexes. Hydrogen peroxide is more reductant in its deprotonated form but it is not defined as a strong reducing agent anyway. In

(37) Karlin, K. D.; Hayes, J. C.; Hutchinson, J. P.; Hyde, J. R.; Zubieta, J. *Inorg. Chim. Acta* **1982**, *64*, L219–L220.
(38) (a) Oikawa, S.; Kurasaki, M.; Kojima, Y.; Kawanishi, S. *Biochemistry* **1995**, *34*, 8763–8770. (b) Oikawa, S.; Kawanishi, S. *Biochemistry* **1996**, *35*, 4584–4590.
(39) Park, J. H.; Gopishetty, S.; Szewczuk, L. M.; Troxel, A. B.; Harvey, R. G.; Penning, T. M. *Chem. Res. Toxicol.* **2005**, *18* (6), 1026–1037.
(40) Yamamoto, K.; Kawanishi, S. *J. Biol. Chem.* **1989**, *264* (26), 15435–15440.
(41) (a) Johnson, G. R. A.; Nazhat, N. B.; Sandalla-Nazhat, R. A. *J. Chem. Soc., Chem. Commun.* **1985**, 407. (b) Johnson, G. R. A.; Nazhat, N. B. *J. Am. Chem. Soc.* **1987**, *109*, 1990–1994. (c) Goldstein, S.; Czapski, G. *J. Free Rad. Biol. Med.* **1985**, *1*, 373. (d) Gorbunova, N. V.; Purmal, A. P.; Skurlatov, Y. I. *Russ. J. Phys. Chem.* **1975**, *49*, 1169.
(42) (a) Walling, C. *Acc. Chem. Res.* **1998**, *31*, 155–157. (b) MacFaul, P. A.; Wayner, D. D. M.; Ingold, K. U. *Acc. Chem. Res.* **1998**, *31*, 159–162. (c) Goldstein, S.; Meyerstein, D. *Acc. Chem. Res.* **1999**, *32*, 547–550.

Scheme 3. Structure of the Known Copper(II) Complexes That Form Cu(II)−Hydroperoxo Intermediates Compared with the Cu(II)−ACC Complexes

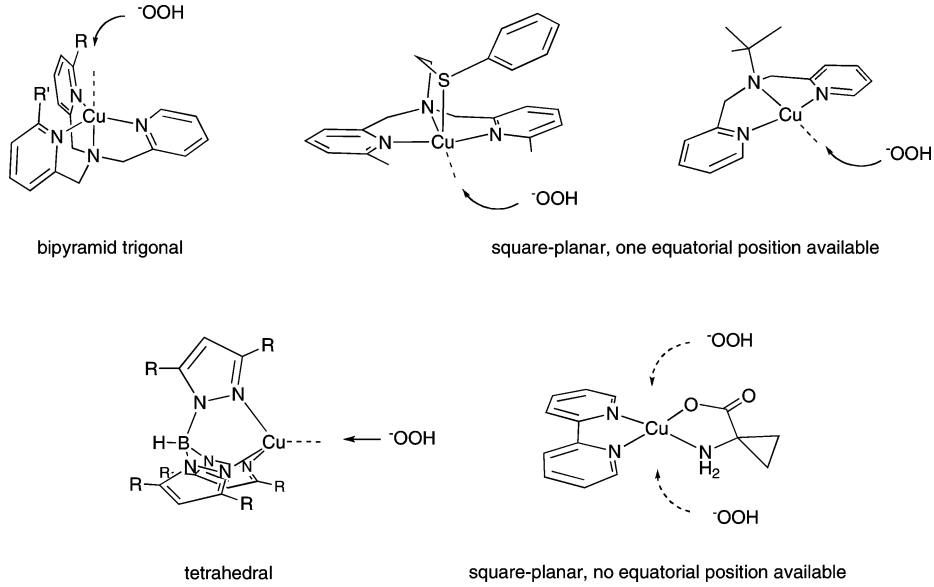

the literatures, the reaction of hydrogen peroxide with Cu(II) complexes has led to the formation of several well identified or postulated Cu(II)-OOH intermediates.[43]

One of these intermediates, the $[Cu(bppa)(OOH)]^+$ complex, has been crystallized by Wada et al.,[43a] and the crystal structure has revealed a copper ion in an axially compressed trigonal-bipyramidal geometry, and the "OOH" group was found in an axial position. A similar geometry is probably found in the Cu(II)−OOH recently described by Karlin et al. with ligands derived from TPA (= tris(2-pyridylmethyl)-amine).[43m,n] Solomon et al.[43i] have reported the hydroperoxo−copper(II) complex with a four-coordinate tetrahedral structure using a trispyrazolylborate ligand. The same kind of intermediate was also described by Buchanan and co-workers with a bisamide functionalized trispyrazolylborate ligand.[43m] Kodera et al.[43b] have described the preparation of the hydroperoxo−copper(II) complex with an N3S-type ligand, which would be a five-coordinated square-pyramidal structure having a phenyl thioether in an apical position. Interestingly, Masuda et al.[43j] have reported the preparation, the characterization, and the reactivity of a Cu(II)−OOH species with a ligand that forced the square-planar geometry around the copper ion. In these two last cases, the hydroperoxo group has been proposed to be coordinated in an equatorial position. These results are summarized in Scheme 3. In the case of tetradentate ligands (top left in Scheme 3), the coordination of the hydroperoxo moiety occurs in an axial position. In the case of square-planar geometry around the copper ion, Itoh et al.[43k] have demonstrated, using DFT calculations, that the hydroperoxo group is preferentially ligated in an equatorial position.

In our case, the geometry around Cu(II) is square-planar, and the four equatorial positions are occupied by ACC and the exogenous ligand. The HOO^- group interacts in an axial position since there are no positions available for its coordination in the equatorial plane. The resulting Cu(II)−OOH species can be readily converted to the corresponding Cu(I) complex through the homolysis of a Cu(II)−OOH bond, probably due to the instability of the formed Cu(II)−OOH complex together with the formation of a stable Cu(I)−NN−amino acid complex, as previously observed by Itoh et al.[36] for the Cu(II)−TEPA complex. One can thus conclude that geometric factors, certainly among other such as electronic or steric factors, would thus play an important role in the orientation toward a Cu(II)−OOH or Cu(I)−OOH intermediate in copper−dioxygen chemistry.

Conclusion

These findings question the proposed mechanism for copper-containing oxygenases such as dopamine β-monooxygenase (DβM) and peptidylglycine α-hydroxylating monooxygenase (PHM). These enzymes contain two independent copper ions at the active site. The reaction mechanism has widely been proposed to proceed via mononuclear

(43) (a) Wada, A.; Harata, M.; Hasegawa, K.; Jitsukawa, K.; Masuda, H.; Mukai, M.; Kitagawa, T.; Einaga, H. *Angew. Chem., Int. Ed.* **1998**, *37* (6), 798–799. (b) Kodera, M.; Kita, T.; Miura, I.; Nakayama, N.; Kawata, T.; Kano, K.; Hirota, S. *J. Am. Chem. Soc.* **2001**, *123*, 7715–7716. (c) Ohta, T.; Tachiyama, T.; Yoshizawa, K.; Yamabe, T.; Uchida, T.; Kitagawa, T. *Inorg. Chem.* **2000**, *39*, 4358–4369. (d) Ohtsu, H.; Itoh, S.; Nagatomo, S.; Kitagawa, T.; Ogo, S.; Watanabe, Y.; Fukuzumi, S. *Chem. Commun.* **2000**, 1051–1052. (e) Ohtsu, H.; Itoh, S.; Nagatomo, S.; Kitagawa, T.; Ogo, S.; Watanabe, Y.; Fukuzumi, F. *Inorg. Chem.* **2001**, *40*, 3200–3207. (f) Ohta, T.; Tachiyama, T.; Yoshizawa, K.; Yamabe, T. *Tetrahedron Lett.* **2000**, *41*, 2581–2585. (g) Chen, P.; Solomon, E. I. *J. Inorg. Biochem.* **2002**, *88*, 368–374. (h) Yamaguchi, S.; Wada, A.; Nagatomo, S.; Kitagawa, T.; Jitsukawa, K.; Masuda, H. *Chem. Lett.* **2004**, *33* (12), 1556–1557. (i) Yamaguchi, S.; Masuda, H. *Sci. Technol. Adv. Mater.* **2005**, *6*, 34–47. (j) Chen, P.; Fujisawa, K.; Solomon, E. I. *J. Am. Chem. Soc.* **2000**, *122*, 10177–10193. (k) Fujii, T.; Naito, A.; Yamaguchi, S.; Wada, A.; Funahashi, Y.; Jitsukawa, K.; Nagatomo, S.; Kitagawa, T.; Masuda, H. *Chem. Commun.* **2003**, 2700–2701. (l) Osako, T.; Nagatomo, S.; Kitagawa, T.; Cramer, C. J.; Itoh, S. *J. Biol. Inorg. Chem.* **2005**, *10*, 581–590. (m) Cheruzel, L. E.; Cecil, M. R.; Edison, S. E.; Mashuta, M. S.; Baldwin, M. J.; Buchanan, R. M. *Inorg. Chem.* **2006**, *45* (8), 3191–3202. (n) Maiti, D.; Sarjeant, N.; Karlin, K. D. *J. Am. Chem. Soc.* **2007**, *129*, 6720–6721. (o) Maiti, D.; Lucas, H. R.; Sarjeant, A. A. N.; Karlin, K. D. *J. Am. Chem. Soc.* **2007**, *129*, 6998–6999.

$Cu-O_2$ species.[44] This copper(II)−superoxo intermediate could be the reactive intermediate involved in H-atom abstraction on the substrate.[45,46] This is supported by the recent work of Masuda et al., who have prepared a copper(II)−hydroperoxo intermediate by reaction of a copper(I) complex with dioxygen *via* a copper(II)−superoxo species.[47] Theoretical support has been provided by Solomon and Chen, who have proposed that a copper(II)−hydroperoxo is then generated by H-atom abstraction by the copper(II)−superoxo species.[48] Karlin and co-workers have suggested that, in DβM and PHM, the hydroxylating agent could be a high-valent CuO species.[49] However, Amzel et al. have also proposed the occurrence of a Cu(I)−hydroperoxo intermediate in the catalytic cycle of PHM.[50] This last hypothesis is supported by the fact that compounds containing a thioether ligand stabilize the Cu(I) redox state,[51] and that the Cu_B ion in PHM, where the oxidation takes place, is ligated by a methionine.

Further work will thus concentrate on elucidating the oxidation mechanism of Cu(II)−ACC systems. Efforts will focus on the characterization of reaction intermediates such as Cu(I)−OOH species. This may provide insight into the mechanism of copper-containing oxygenases but also, possibly, on the catalytic mechanism of ACC oxidase. Indeed, ACCO is an associate member of a superfamily of iron(II)-containing oxidases and oxygenases that catalyze a wide range of oxidation reactions, most of them utilizing 2-oxoglutarate as a cosubstrate (which is transformed into succinate and carbon dioxide). Although ACCO uses ascorbate and not α-ketoglutarate as a cofactor, it presents strong sequence and structural analogies with some members of this family.[52] Moreover, very recently, Tolman et al. have described a copper(I)−α-ketoglutarate complex that can react with dioxygen to perform arene hydroxylation.[53] This system, being a copper-containing model of α-ketoglutarate-dependent oxygenases, emphasizes the parallel that might be established between copper and iron systems.

Acknowledgment. The authors thank Prof. Eric Saint-Aman (Grenoble, France) for assistance with electrochemical experiments and Dr. Catherine Belle, Prof. Shinobu Itoh (Osaka, Japan), and Prof. Masahito Kodera (Kyoto, Japan) for interesting discussions. This work was performed within the framework of a CNRS−JSPS exchange program and thanks to the "Collège Doctoral Franco-Japonais". A.R. is also thankful for the financial support of the Hungarian National Research Fund: OTKA K-72781.

Supporting Information Available: EPR experimental and simulated spectra for **1b**, **2a**, and **3a**. ORTEP drawing and atomic coordinates of [Cu(I)(2,2′-bipyridine)(ACC)] and [Cu(I)(2,2′-bipyridine)(ACC)(OOH)]$^-$ obtained by DFT geometry optimization. Crystal structure of **1af**. CIF files for complexes **2a**, **3a**, **1b** and **1af**. This material is available free of charge via the Internet at http://pubs.acs.org.

IC702303G

(44) Prigge, S. T.; Eipper, B. A.; Mains, R. E.; Amzel, L. M. *Science* **2004**, *304*, 864–867.
(45) Klinman, J. P. *Chem. Rev.* **1996**, *96*, 2541–2561.
(46) Bauman, A. T.; Yulk, E. T.; Alkevich, K.; McCormack, A. L.; Blackburn, N. J. *J. Biol. Chem.* **2006**, *281* (7), 4190–4198.
(47) Fujii, T.; Yamaguchi, S.; Funahashi, Y.; Ozawa, T.; Tosha, T.; Kitagawa, T.; Masuda, H. *Chem. Commun.* **2006**, 4428–4430.
(48) Chen, P.; Solomon, E. I. *J. Am. Chem. Soc.* **2004**, *126*, 4991–5000.
(49) Maiti, D.; Lee, D.-H.; Gaoutchenova, K.; Würtele, C.; Holthausen, M. C.; Sarjeant, A. A. N.; Sundermeyer, J.; Schindler, S.; Karlin, K. D. *Angew. Chem., Int. Ed.* **2007**, *46*, 1–5.
(50) Prigge, S. T.; Kolhekar, A. S.; Eipper, B. A.; Mains, R. E.; Amzel, L. M. *Nat. Struct. Biol.* **1999**, *6* (10), 976–983.
(51) Casella, L.; Gulotti, M.; Bartosek, M.; Pallanza, G.; Laurenti, E. *J. Chem. Soc., Chem. Commun.* **1991**, 1235–1237.
(52) Clifton, I. J.; McDonough, M. A.; Ehrismann, D.; Kershaw, N. J.; Granatino, N.; Schofield, C. J. *J. Inorg. Biochem.* **2006**, *100*, 644–669.
(53) Hong, S.; Huber, S. M.; Gagliardi, L.; Cramer, C. C.; Tolman, W. B. *J. Am. Chem. Soc.* **2007**, *129*, 14190–14192.